

Article

A Graphical Method for Combined Heat Pump and Indirect Heat Recovery Integration

Raphael Agner ^{1,*}, Benjamin H. Y. Ong ^{1,†}, Jan A. Stampfli ¹, Pierre Krummenacher ² and Beat Wellig ¹

¹ Competence Center Thermal Energy Systems and Process Engineering, Lucerne University of Applied Sciences and Arts, Technikumstrasse 21, 6048 Horw, Switzerland; benjamin.ong@hslu.ch (B.H.Y.O.); jan.stampfli@hslu.ch (J.A.S.); beat.wellig@hslu.ch (B.W.)

² Institut de Génie Thermique, The School of Management and Engineering Vaud, Avenue des Sports 20, 1401 Yverdon-les-Bains, Switzerland; pierre.krummenacher@heig-vd.ch

* Correspondence: raphael.agner@hslu.ch

† These authors contributed equally to this work.

Abstract: Industrial sectors are improving their energy efficiency and increasing their share of renewables for heating and cooling demands by using lower emission technologies. One specific approach to help achieve these targets is the integration of heat pumps (HPs) in industrial processes. However, due to the temporal variation of the heating and cooling requirements in non-continuous processes, the integration of HP is challenging. In this paper, a structured method for the design of HP integration is proposed. The method implements an engineer-centred workflow that extends the concept of the Indirect Source Sink Profile (ISSP) to HP integration. For this purpose, an adapted Grand Composite Curve is derived from the ISSP. This ensures correct HP integration across the pinch while maintaining the temperature lift of the HP small. The proposed workflow is applied to a demonstration case study and a case study from industry. In both cases, the resulting system with integrated HP enables the elimination of hot utility demand and significantly reduces cold utility demands. The static paybacks of the proposed solutions are in the range of 4.5 to 5 year.

Keywords: energy optimisation; process integration; heat pump; thermal energy storage; electrification



Citation: Agner, R.; Ong, B.H.Y.; Stampfli, J.A.; Krummenacher, P.; Wellig, B. A Graphical Method for Combined Heat Pump and Indirect Heat Recovery Integration. *Energies* **2022**, *15*, 2829. <https://doi.org/10.3390/en15082829>

Academic Editors: Petar Varbanov, Xuexiu Jia and Xue-Chao Wang

Received: 14 March 2022

Accepted: 9 April 2022

Published: 13 April 2022

Publisher's Note: MDPI stays neutral with regard to jurisdictional claims in published maps and institutional affiliations.



Copyright: © 2022 by the authors. Licensee MDPI, Basel, Switzerland. This article is an open access article distributed under the terms and conditions of the Creative Commons Attribution (CC BY) license (<https://creativecommons.org/licenses/by/4.0/>).

1. Introduction

Today, industrial companies must meet a wide range of requirements. Generally, processes should exhibit maximum economic efficiency alongside high energy efficiency and low emissions. In the medium to long term, rising energy prices and incentive taxes will make it essential that energy-intensive companies increase their energy efficiency in order to remain competitive. In recent years, industry has made great efforts in the field of energy efficiency; however, considerable potential for increasing efficiency remains. One specific approach to help achieve targets is the integration of heat pumps (HPs) in industrial processes. Depending on the emission factor of electric energy, the integration of HPs is a key enabler of decarbonisation of the heating and cooling supply. Furthermore, with the use of HPs, heat recovery (HR) can be increased and the required utilities reduced in turn.

In this work, Pinch Analysis (PA) is used to integrate heat pumps into industrial processes. PA allows for the analysis of heat recovery potential and HP integration. Townsend and Linnhoff [1] defined the rules for HP integration in PA for continuous processes using the Grand Composite Curve (GCC). Hindmarsh et al. [2] showed the influence of the evaporating temperature of refrigeration systems on their power consumption by integrating HP across the Pinch. Wallin et al. [3] developed a method for determining the optimal temperature level and optimal HP size and type using composite curves. Their work was further extended using the GCC [4]. However, it should be noted that true temperatures have to be used instead of the shifted temperatures in the GCCs when calculating the

actual temperature lift of HPs, as this affects the performance of the HP. The graphical approach using GCC for HP integration has been applied to several case studies, including a whiskey production process [5], a cheese factory [6], a biomass gasification process [7], and a confectionery production plant [8]. Schlosser et al. [9] developed the Heat Pump Bridge Analysis (HPBA) for the efficient integration of heat pumps using Modified Energy Transfer Diagram [10]. The Modified Energy Transfer Diagram is an adaptation of the GCC to represent existing heat exchangers (HEXs) in the network. Without the assumption that the remaining heat recovery potential is to be exploited (as in the GCC), the HPBA is able to increase heat recovery rate and reduce temperature increase in the HP.

For various reasons (irregular production schedules, high demand for flexibility, product changes, different workloads, interruptions for cleaning, etc.), many industrial processes are non-continuous in nature. In non-continuous processes, direct HR is usually limited due to the different process schedules of the single streams [11]. On account of temporal variations in the heating and cooling requirements for integration of HPs, their use in non-continuous processes presents particular difficulties in selecting an HP with appropriate operational characteristics (such as feasible evaporation and condensation temperature ranges) as well in their optimal placements across the Pinch Point [8]. Despite this, such systems have been shown to be economically viable (e.g., waste HR from batch reactor systems [12]), and a small though growing number of non-continuous process HP integration case studies [13].

In order to smooth out fluctuations in power consumption, thermal energy storage (TES) is usually integrated in addition to HP. Glembin et al. [14] demonstrated a methodology for TES integration in a solar thermal power system including an HP. Energy demand can be reduced by increasing the number of temperature levels at which heat is stored or delivered. Another approach for TES integration in HP systems was developed by Floss and Hofmann [15], where the authors studied the efficiency of an HP based on the arrangement of the TES integration into the HP either in parallel or in series.

The systematic integration of HP and TES into non-continuous processes is a major challenge in terms of conceptual design, layout, and planning, as well as for operation. Multiple challenges faced by the industry in the integration of HP have prevented the widespread adoption of the technology [16]. Becker et al. [17] developed a method combining the Time Average Model (TAM) with restricted matches [18] to optimally integrate HPs in a cheese factory. The same method can be applied including specific process characteristics. Becker and Maréchal [19] carried out a multi-objective optimisation of operating and capital costs for different combinations of HP configurations implemented in non-continuous processes using the Time Slice Model (TSM) and TES. Schlosser et al. [20] designed an intelligent HP and TES system using a standby control system to deal with the complicated and highly variable heat sources and sinks in manufacturing systems. By simultaneously combining HP and TES systems with standby control systems, the authors were able to minimise energy demands and maximise waste HR. Prendl et al. [21] carried out a mathematical optimisation to simultaneously integrate HP and storage into multi-period superstructure formulation. Their work built on the optimisation superstructure [22] with a convex linearisation of the cost function based on the size and energy consumption of HP [23], with a continuation to extend the work by introducing additional storage considerations to allow and enhance HR between operating cases. Various approaches from the literature can enable complex analysis of non-continuous processes, although these require a high level of user knowledge as well as substantial computation power and time, leading to optimal though largely impractical results, e.g., a plant design with multiple splits. Stampfli et al. [24] combined PA with mathematical programming techniques to allow for the practical engineering flexibility to integrate HP in non-continuous processes while avoiding long computation times. The authors restricted the solution space using PA and reduced the complexity of the problem to a nonlinear programming problem involving optimizing the temperature level in the HP system. The work carried out by Stampfli et al. [24] considered HP integration in a utility system; however, Becker et al. [17]

have shown that direct heat exchange between the process and the HP yields higher efficiency. Integrating the HP system directly into the process can reduce temperature increase in the HP, meaning that less heat is exchanged between the process streams and the HP.

1.1. The Indirect Source Sink Profile

To exploit the indirect heat recovery (IHR) potential of processes, ref. [25] TAM-based methods are used for analysis. The TAM represents the average heat flow over a repetitive time period of the process, called the streamwise repeated operation period (SROP). As it disregards the scheduling of the process, the TAM provides an upper bound for the direct and IHR potential of a process. In this work, the Indirect Source Sink Profile (ISSP) is used to address the non-continuous nature of industrial processes. The ISSP was introduced by Olsen et al. [26], and is based on the development of Krummenacher and Favrat [27] and Walmsley et al. [28]. Krummenacher and Favrat [27] developed a methodology for heat integration of batch processes based on TAM. Walmsley et al. [28] built on this methodology to design HR loops for IHR of semi-continuous processes, where it accounts for shifting of stream temperatures based on the heat transfer coefficients. The ISSP is built based on both these works, with the streams in the ISSP rearranged in priority relative to one another using temperature shifting. This ensures better distribution of capital costs related to the HR HEX. Streams with “high attractiveness for IHR” are shifted less; therefore, streams that have longer duration or have larger film heat transfer coefficient are shifted less in the ISSP, leading to higher IHR utilisation. In addition, the ISSP method ensures that the resulting storage system is technically feasible, the heat balance is guaranteed, and the required amount of storage and HEXes are as low as possible. The latter objective is enabled by the assignment zone (AZ) algorithm for the ISSP, which was introduced by Abdelouadoud et al. [29]. AZs prescribe the degree of freedom in terms of the enthalpy to be stored within one storage intermediate loop (IL) and the temperatures at which ILs are to be operated. The sizing of the storage volumes is based on the sequence of the loading and unloading phases of the TSM. Figure 1 illustrates an exemplary ISSP with corresponding storage ILs. The ILs are displayed as black lines, directly showing the extent to which the IHR of each IL is realized and at what temperature levels the storage operates. Furthermore, the Heat Exchanger and Storage Network (HESN) is directly derived from the ISSP, as it matches the hot and cold streams to their respective ILs. While the ISSP method enables IHR, it does not, to date, include any functionality to assist in the integration of HPs.

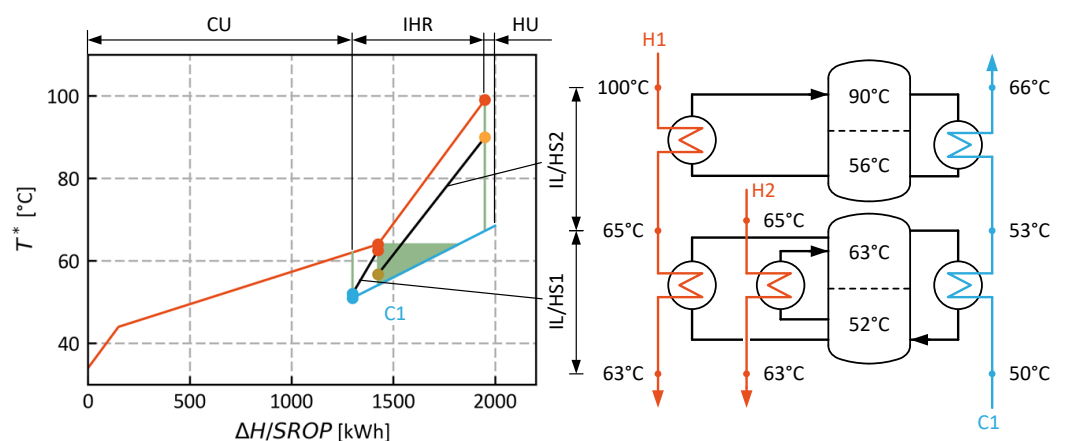


Figure 1. Example of an ISSP (red lines: Source Profile and source streams, blue lines: Sink Profile and sink stream) with three Assignment Zones (AZs) (green lines at beginning and end of IHR and green area in the middle) and the resulting two storage intermediate loops (ILs). The chosen design target is realised with two two-layer stratified heat storage (HS).

1.2. Problem Statement and Aims

The systematic integration of a heat pump and thermal energy storage into non-continuous processes is a major challenge in terms of conceptual design, layout, and planning, as well as operation. In addition to the aforementioned literature on HP integration using PA, HP integration in non-continuous processes is usually formulated in mathematical programming as a mixed-integer nonlinear problem (MINLP). Although mathematical programming provides a wide variable solution space and optimal design, it tends to involve high computation times and requires specialised engineers. This means that while mathematical programming may lead to optimal results, it may not always lead to practical results. In order to achieve field deployment of HPs in non-continuous processes, engineers must have tools at hand that help to produce practical system designs with potential for widespread adoption involving an acceptable level of training. The aim of this work is to address the challenges facing HP integration in non-continuous processes using a method that is:

1. Practice-oriented: solutions that are applicable in industry;
2. Engineer/user-centric: user-friendly workflow where engineers/users are able to follow through and control the solution;
3. Easily adoptable: low degree of user specialization conferring widespread adaptability along with acceptably low computation times.

This work aims to extend the ISSP method for the integration of HPs in combination with TES (HPTES system) into non-continuous processes in order to improve energy efficiency. There is currently a gap in the literature in that there is no method to evaluate the integration of HPs combined with IHR systems or separate from them. Theoretically, TES requirements can be reduced in a combined HP and IHR system. However, with a separate HP system the HP is less interconnected with the processes and may be more robust in operation. The novelties introduced in this paper are:

1. Introduction of the inverted residual ISSP;
2. Derivation of the ISSP-based adapted GCC.

2. Methodology

2.1. Overall Workflow

This paper develops a workflow that enables the practical integration of a heat pump and thermal energy storage system into non-continuous processes. The work provides a structured framework for HP integration with TES into non-continuous processes. Figure 2 shows an overview of the proposed workflow.

Embedded in the workflow is existing the PA [30] for direct heat recovery and the extension of the ISSP. The workflow is a variant based approach. A solution variant is composed of an indirect heat recovery overlap selected by the user in the ISSP, a choice of the HP integration pathway in the workflow, and a certain HP-placement. The engineer maintains control of decisions at all stages and can decide which solution variants to evaluate and influence. A crucial element of the analysis and optimisation involves the integration of the HP and associated HESN into the system; the overall problem of HP integration in non-continuous processes may cause changes in the HESN topology, as heat exchanger matches between streams are dependent on many factors including HP placement. One key assumption made in this study is that the HP operates continuously and at fixed evaporator and condenser temperatures.

Illustrations using the results of the analysis of the Demonstration Case (introduced in Section 3.1) are used to demonstrate the methodology. This is intended to illustrate the difference between the two pathways in the design of the HPTES system. A detailed explanation of the results can be found in Section 4.1.

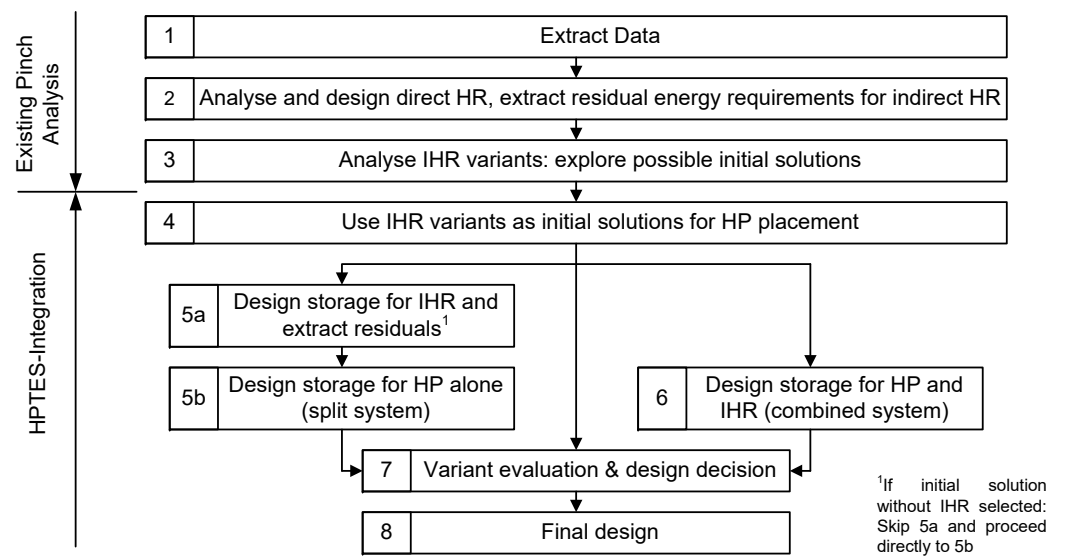


Figure 2. Workflow for the integration of HPTES system into non-continuous processes.

2.2. Data Extraction and Direct Heat Recovery (Steps 1 and 2)

For conducting a PA, the heating and cooling demands of the process (known as process requirements) have to be identified. Extracting these data from the physical plant in order to define the heating and cooling requirements of the process is the first step in any PA. The result of data extraction is a listing of the process requirements, including their scheduling; this is called the stream table. To achieve this goal, assumptions and simplifications must be made by the user in order to compile the vast extent of process information into a representative set of process requirements. When analysing the process, an engineer will typically have to first identify the types of processes present, the range of products (different operating cases), and the different production lines (conditions and schedules). Further information on data extraction is available in Klemeš and Varbanov [31] and in Brunner and Kruppenacher [32].

After the process stream table is defined, the energy targets for direct HR within the individual time slices can be identified using Composite Curves. This allows for quick identification of the potential scope for energy saving at an early stage. With the energy targets defined, the actual design of the heat exchanger network (HEN) can be carried out for direct HR. Direct HR is only realized as an HEN for streams with inherently concurrent schedules, as schedule variations can prevent these measures from operating. The shares of the streams that are heated or cooled with this newly designed direct HR measures are then subtracted from the stream table, and only their remainders are used for further analysis.

2.3. Indirect Heat Recovery (Steps 3 and 4)

The remaining heating and cooling demands for the IHR are then analysed using the ISSP. The streams within the ISSP are already shifted to ensure practicality and improve the distribution of the investment cost according to their attractiveness for IHR. The streams are rearranged by shifting the supply and target temperatures based on the calculated stream-specific $\Delta T_{min,s}$ contribution shown in Equation (1) [26]

$$\Delta T_{min,s} = f_p \left(\frac{1}{U_s t_s} \right)^y \quad \text{with : } f_p = \max[(U_s t_s)^y] \Delta T_{min,ov} \quad (1)$$

where U_s is the overall heat transfer coefficient between the IL fluid and the process stream and t_s is the duration of the stream in the TSM. The variable f_p is a proportionality constant that is determined beforehand based on a user-specified minimum overall temperature difference, $\Delta T_{min,ov}$. The y -exponent influences the magnitude of temperature shifting. Once an individual stream's $\Delta T_{min,s}$ contribution is determined, it is either subtracted from

the stream supply or added to the target temperature. The ISSP can then be constructed in a composite manner using the new shifted stream temperatures. The ISSP identifies the maximum potential of possible IHR and shows the amount of residual heat loads above and below the Pinch present, which may be used for HP integration after the extent of IHR is determined. Figure 3 shows ISSPs with three different extents of overlap: 0 kWh (i.e., no IHR), IHR of 80 kWh, and IHR of 140 kWh (all with $\Delta T_{min,s} = 1$ K). The user has to select the extent of overlap as the initial solution for HP integration in Step 4.

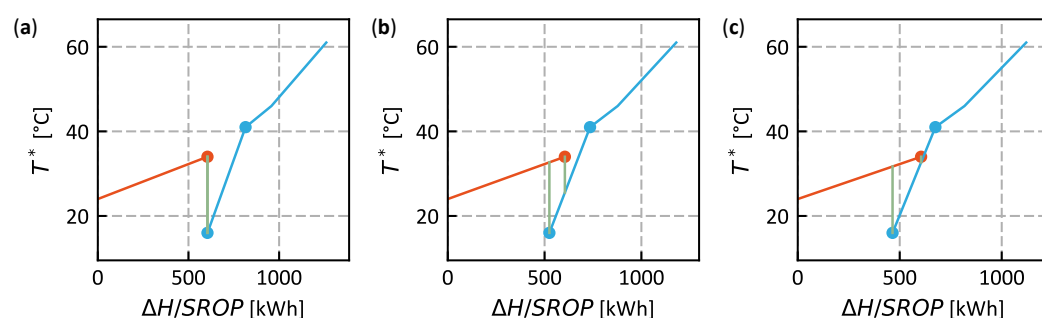


Figure 3. ISSP with different IHR initial solutions for the demonstration case: (a) no IHR; (b) with 80 kWh IHR; and (c) with 140 kWh IHR.

In Step 4, possible IHR solutions must be chosen for further evaluation regarding their HP integration potential. These selected IHR solutions are used as the benchmark for evaluation of the final variant in Step 7. This enables the comparison of the economic potential of an HP integrated final system against both the initial situation and the IHR solution alone. After the selection of the initial solution, there are two pathways for integration of HP in the workflow: (i) integration of the HP into its own HESN in addition to the IHR HESN (denominated as a split-system design) and (ii) the integration of the HP into the same HESN used for IHR (denominated as a combined system design). The first pathway leads to the execution of Steps 5a and 5b, while the latter leads to the execution of Step 6. Solution variants for the HP integration must be selected such that the initial IHR solution allows for a low complexity, i.e., low amount of equipment to be installed, as well as less easily quantifiable aspects such as expected unknown schedule variations, etc. This selection is further detailed in Steps 5 and 6.

2.4. Indirect Heat Recovery Solution with Separate Heat Pump System (Step 5)

Using the selected initial solution, Step 5 designs the IHR solution with a separate HPTES system. Figure 4a shows the placed storage for the selected degree of IHR. The residual heating and cooling demands (the share of streams not included in the IHR) are then extracted to construct a new ISSP where no more IHR overlap is applied (Figure 4b). The residual heating and cooling demands are to be covered by the HP or utility entirely. In order to dimension the HP, the residual ISSP is converted to the inverted residual ISSP, as shown in Figure 4c. In Figure 4c, the source profile (hot composite curve) is inverted in its enthalpy coordinates. This allows the heating and cooling demands to be shown in a similar way as in the GCC, and thus enables users to place the HP as they would with a GCC. The inverted residual ISSP is distinguished from the GCC in that a GCC shows the net heat deficit and surplus after HR, while the inverted residual ISSP shows the gross heat deficit or surplus, i.e., with no further HR implementation.

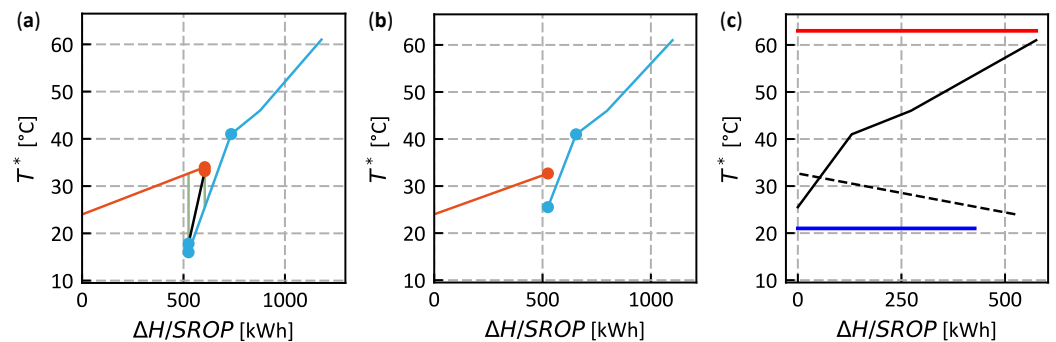


Figure 4. Design procedure of split IHR and HPTES system: (a) design of HESN for IHR solution; (b) residuals of ISSP after design of IHR solution; (c) inverted residual ISSP for HP placement with the residual heating demand (solid black line), residual cooling demand (dashed black line), and HP evaporator and condenser (solid blue and red line, respectively).

The HP is placed in Step 5b. The HP is modelled as a Carnot cycle with a constant second law efficiency according to Equation (2), where ζ_c is the second law efficiency of the Carnot cycle, T_{cond}^* and T_{evap}^* are the ISSP-shifted condensation and evaporation temperature, and ΔT_{cond} and ΔT_{evap} are the condensation and evaporation temperature shift for the ISSP. The shift temperatures must be set to typical values of the difference between the medium outlet and the condensation and evaporation temperature, respectively, with T_{cond} and T_{evap} being the real condensation and evaporation temperatures, respectively.

$$COP = \zeta_c \frac{T_{cond}}{T_{cond} - T_{evap}} = \zeta_c \frac{T_{cond}^* + \Delta T_{cond}}{(T_{cond}^* + \Delta T_{cond}) - (T_{evap}^* - \Delta T_{evap})} = \frac{\dot{Q}_{cond}}{P_{el}} \quad (2)$$

Once the HP is placed (temperatures and duty determined) using the inverted residual ISSP, the sizing of the HESN can be carried out using the ISSP and the underlying TSM, enabling the later variant evaluation in Step 7.

2.5. Combined Indirect Heat Recovery and Heat Pump System (Step 6)

As an alternative to the aforementioned pathway in Step 5, it is possible to find solutions where the HP and IHR can be combined within the same HESN (Step 6). In a combined system, IHR is desired and the net heat deficit or surplus after IHR needs to be known for HP placement. For continuous processes, the GCC derived by Townsend and Linnhoff [33] shows the net heat deficit and surplus of a process. Applying this derivation to the ISSP would, however, lead to very conservative HP placement. The ISSP poses additional challenges for the derivation of a suitable GCC. First, the streams within the ISSP are already shifted. As previously mentioned, it is often not desirable to achieve the maximum IHR overlap for an IHR solution, as this requires a large number of AZs in the ISSP. Furthermore, when there is a small overlap in the ISSP, the temperature difference at the Pinch is large and the temperature shifting of the ISSP would consequently be large as well if the GCC of the ISSP was calculated as it is for continuous processes, ultimately leading to an artificially increased HP temperature and poor HP efficiency.

Because of the aforementioned challenges, we propose the calculation of an adapted GCC of the ISSP. While the CCs are shifted when calculating the GCC for continuous processes, the adapted GCC for the ISSP is calculated without temperature shifting of the ISSP. This is possible because the ISSP is already shifted during its generation. Figure 5 shows the difference in the potential real HP condensation temperature reduction and evaporation temperature increase between the calculation of the GCC with (red lines) and without (black lines) shifting of the ISSP.

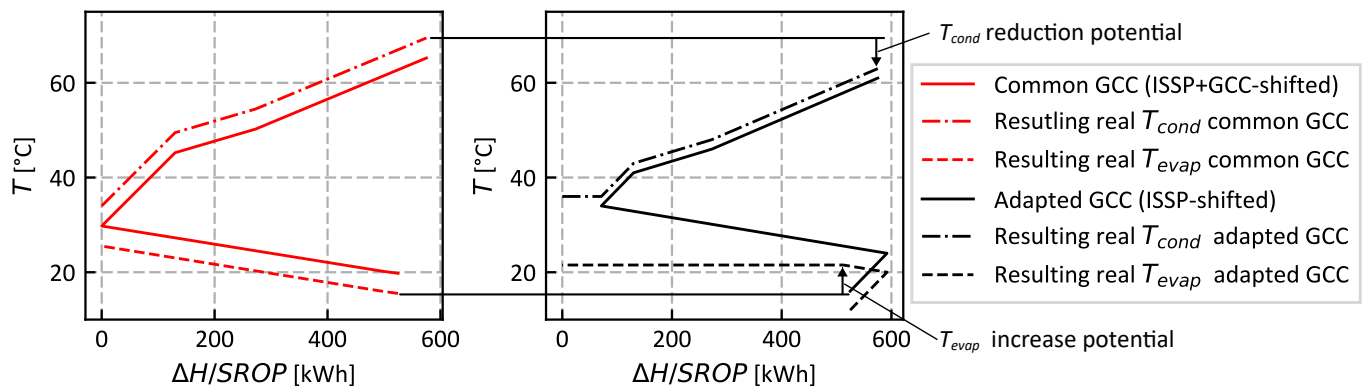


Figure 5. Resulting real T_{cond} and T_{evap} of the correctly integrated HP if (i) the HP is integrated with GCC as calculated for continuous processes (Townsend and Linnhoff [1], red lines) and (ii) the HP is integrated with the adapted GCC (black lines). The potential reduction in temperature increase when using the proposed adapted GCC is highlighted. Data taken from Demonstration Case with an IHR overlap of 80 kWh.

The adapted GCC shows the desired net heat surplus and deficit of the process. This ensures that the HP is not operated at unnecessary high temperature increases while ensuring thermodynamical feasibility thanks to the individual shifting of the streams in the ISSP.

Without the temperature shifting of the ISSP in the adapted GCC calculation, however, it is necessary to impose limits to allow the HP to operate across the Pinch. The evaporator must extract heat from the subsystem below the Pinch and the condenser must add heat to the subsystem above the Pinch. To achieve this, temperature limits on the shifted evaporation and condensation temperatures are required, as illustrated in Figure 6a. These limits are the temperatures of the source and the sink profile at the Pinch. The temperature limits in the adapted GCC are shown as the shaded area between the minimum condensation and maximum evaporation temperature (Figure 6b). The evaporator (T_{evap}^*) has to be placed below this area, and the condenser (T_{cond}^*) above this area.

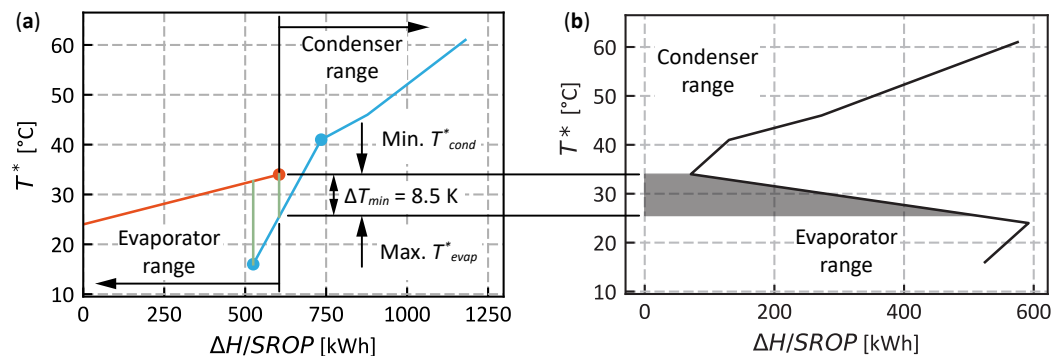


Figure 6. (a) ISSP of the demonstration case with IHR of 80 kWh. The enthalpy ranges of the evaporator and condenser are marked with the corresponding maximum evaporation and minimum condensation temperature. (b) Resulting adapted GCC, including restricted temperature range.

The integration of the HP often leads to the requirement of additional AZs. Every additional AZ should be understood as an increase in the complexity of the system, as additional volume storage units (VSUs, ref. [26]) are required. A VSU typically represents a temperature layer in the storage system. This work only considers stratified storage with two layers. As the integration of an HP changes the topology of the system, different placements can lead to different numbers of AZs. To support the placement of the HP, an enumeration of the feasible HP placement options is performed. This enumeration evaluates the resulting number of AZs if an HP is placed in one of the feasible regions in

the adapted GCC (Figure 6b). The AZ algorithm [29] is applied in a brute force approach. This brute force enumeration evaluates HP placement options starting from the condenser placement. The corresponding feasible evaporation temperatures are evaluated for each condenser placement. The HP characteristics are calculated according to Equation (2). The result of this procedure is shown in Figure 7a,b for the 80 kWh IHR overlap and 140 kWh IHR overlap variants, respectively. The adapted GCC includes the restricted area, which, as shown in Figure 7b, is small due to the small remaining temperature difference between the ISSP at 140 kWh IHR overlap.

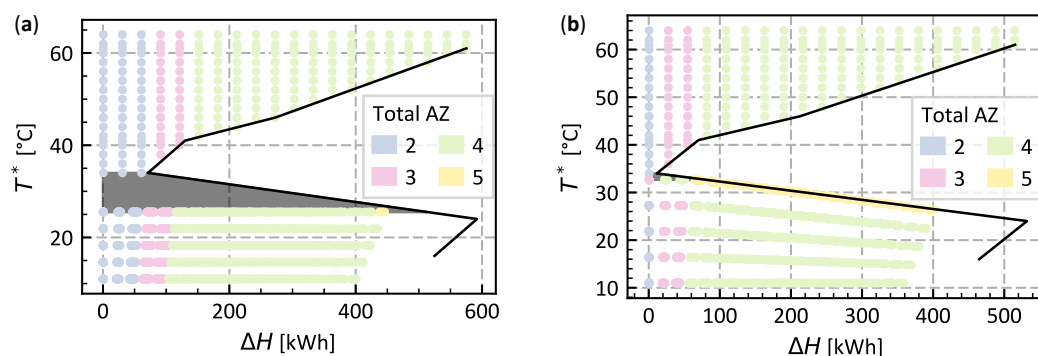


Figure 7. Adapted GCC with resulting number of AZs in the overall system depending on HP placement (AZ-information): (a) for 80 kWh initial solution and (b) for 140 kWh initial solution.

The graph shows the condenser range and the minimum required number of AZs for the respective condenser placement. In the evaporator range (below the Pinch), it shows the resulting number of AZs for the corresponding condenser and evaporator placement. The proposed adapted GCC with AZ information shows whether the HP temperatures or duties have an impact on the required number of AZs, and thus on the complexity of the system. The number of AZs shown in the adapted GCC with AZ information must then be compared to the required number of AZs in the IHR initial solution. HP integrated systems should always have more than two AZs, otherwise the HP would be operating with the condenser and evaporator in the same intermediate storage loop.

2.6. Variant Evaluation (Steps 7 and 8)

After the integration of the HPTES system, Step 7 compares the different solution variants. Several factors are considered, including technical feasibility and controllability of the system, investment cost, and resulting energy cost, as well as economic requirements such as payback period. While technical feasibility requires engineering judgment, investment cost and energy cost estimates can be calculated by the ISSP [26]. The ISSP with the AZ-algorithm provides the boundary conditions for VSU placement. Thereafter, the user has to select the enthalpy coordinates of each VSU in the ISSP as well as the temperatures of the VSUs. Once these parameters are selected, the investment cost of the solution can be determined. The evaluation of the equipment cost is detailed in Olsen et al. [26].

3. Case Studies

This section presents two case studies. Case 1, the Demonstration Case, is a generated case study to guide readers through an explanation of the methodology. Case 2, which is a case from the dairy industry, shows the application of the method to a real case.

3.1. Case 1: Demonstration Case

The demonstration case contains three streams, shown in Table 1. The process is operated for 1500 batches per year, resulting in a total operation duration of 6000 h/y.

Table 1. Process stream table of Case 1.

Stream Name	T_{α} [°C]	T_{ω} [°C]	\dot{m} [kg/s]	c_p [kJ/(kgK)]	h [W/(m ² K)]	t_{start} [h]	t_{end} [h]
H1	35	25	7.2	4.2	2000	0	2
C1	15	45	1	4.2	2000	2	4
C2	40	60	2.4	4.2	2000	1	3

Table 2 lists the utility costs used in the case study; the values represent typical values for a smaller company in the Swiss dairy industry based on the experience of the authors.

Table 2. Cost function and utility costs for analysis of demonstration case.

Utility	Cost [CHF/MWh]
HU	80
CU	35
Electricity	120

3.2. Case 2: Industry Case

This case study is based on data from a PA conducted in the Swiss dairy industry. The process is operated for 339 batches (days) per year. Each stream occurs only during a certain time period from t_{start} to t_{end} . The process requirements are summarised in Table 3, showing a representative day of production. The film heat transfer coefficient h is 2000 W/(m²K) for all streams.

Table 3. Process stream table of Case 2. Streams with multiple periods of occurrence during one batch are denominated by the ending _P.

Streams	T_{α} [°C]	T_{ω} [°C]	\dot{m} [kg/s]	c_p [kJ/(kg K)]	t_{start} [h]	t_{end} [h]
Coagulator Supply_P1	30	42	4.2	4.2	0	3
Coagulator Supply_P2	30	42	4.2	4.2	4	11
Coagulator Supply_P3	30	42	4.2	4.2	12	18
Coagulator Supply_P4	30	42	4.2	4.2	20	24
Coagulator HR_P1	16	31.2	4.7	4.2	5.5	6.5
Coagulator HR_P2	16	31.2	4.7	4.2	13.5	14.5
Coagulator HR_P3	16	31.2	4.7	4.2	20.5	22.5
Bulkhead Cooling_P1	19.4	10	6.3	3.85	0	3
Bulkhead Cooling_P2	31.7	10	6.3	3.85	3	4
Bulkhead Cooling_P3	19.4	10	6.3	3.85	4	5.5
Bulkhead Cooling_P4	19.4	10	6.3	3.85	6.5	11
Bulkhead Cooling_P5	31.7	10	6.3	3.85	11	12
Bulkhead Cooling_P6	19.4	10	6.3	3.85	12	13.5
Bulkhead Cooling_P7	19.4	10	6.3	3.85	14.5	18
Bulkhead Cooling_P8	31.7	10	6.3	3.85	18	20
Bulkhead Cooling_P9	19.4	10	6.3	3.85	20	20.5
Bulkhead Cooling_P10	19.4	10	6.3	3.85	22.5	24
Milk Treatment_P1	30	40	6.9	4.2	0	2
Milk Treatment_P2	30	40	6.9	4.2	22	24
Cream Ripener_P1	19.8	22	8.5	4.2	16	20
Cream Ripener_P2	19.8	22	8.5	4.2	21	24
Cream Ripener_P3	19.8	22	8.5	4.2	0	1
Cottage cheese wash water_P1	50	20	5	4.2	8	9
Cottage cheese wash water_P2	50	20	5	4.2	10	11

The stream “Cottage cheese wash water” is a soft stream and accordingly causes no cold utility cost.

Table 4 lists the utility costs of Case 2.

Table 4. Utility costs of Case 2; HU and CU are the hot and cold utilities.

Utility	Cost [CHF/MWh]
HU	64
CU	30
Electricity	111

3.3. Common Boundary Conditions

For the economic analysis, the equipment pricing used is listed in Table 5, which is based on Swiss market data [34]; A is the HEX area in m^2 , V_{TES} is the volume of the TES in m^3 , and \dot{Q}_{cond} is the heating capacity of the HP in kW. The economic parameters used for evaluation of the total annual cost (TAC) include 10 year depreciation and an interest rate of 6%.

Table 5. Equipment cost functions for analysis.

Equipment	Cost Function
HEX	$8 \text{ kCHF} + 17.5 \text{ kCHF} \cdot \left(\frac{A}{40 \text{ m}^2}\right)^{0.67}$
TES	$1.5 \frac{\text{kCHF}}{\text{m}^3} \cdot V_{TES}$
HP	$148 \text{ kCHF} \cdot \left(\frac{\dot{Q}_{HP,cond}}{100 \text{ kW}}\right)^{0.42}$

For the integration of the HP, $\Delta T_{cond} = 2 \text{ K}$ and $\Delta T_{evap} = 4 \text{ K}$ are used for Equation (2). These values represent typical operation characteristics when an HP is operated at its design point, and were chosen based on the experience of the authors. The second law efficiency value of $\zeta_c = 0.55$ is used as a typical value.

4. Results

Following the proposed workflow (Figure 2), different options for HP and TES (HPTES) integration for both case studies are detailed in the following sections.

4.1. Case 1: Demonstration Case

4.1.1. Data Extraction and Direct Heat Recovery (Steps 1 and 2)

Starting with the compiled process data, the analysis of direct HR shows that there is no potential for direct HR in this case. The scheduling of the heat source (H1) does not match that of a thermodynamically feasible heat sink (C1).

4.1.2. Indirect Heat Recovery Possibilities and Initial Solution (Steps 3 and 4)

The resulting ISSP for the case study is presented in Figure 3. For the shifting of the streams within the ISSP, the following default parameters were used: $\Delta T_{min,ov} = 1 \text{ K}$, Bandwidth exponent $y = 0.9$ (See Equation (1)) [26].

The three overlaps are shown to illustrate three different scenarios. One is close to the maximum potentials IHR (140 kWh), one represents a moderate IHR (80 kWh), and the third no IHR. Out of the three overlaps an IHR of 80 kWh, as shown in Figure 3b, was selected to proceed to Step 5a and 5b of the workflow. This was because the temperature approaches between the ISSP and potential storage were seen to be the most practical feasible. The solution with 80 kWh of IHR overlap is thus the first solution variant (Variant 1), and serves as a benchmark to evaluate whether HP integration in addition to TES integration is economically viable. The schematic of Variant 1 is presented in the top part of Figure 8 within the dotted rectangle.

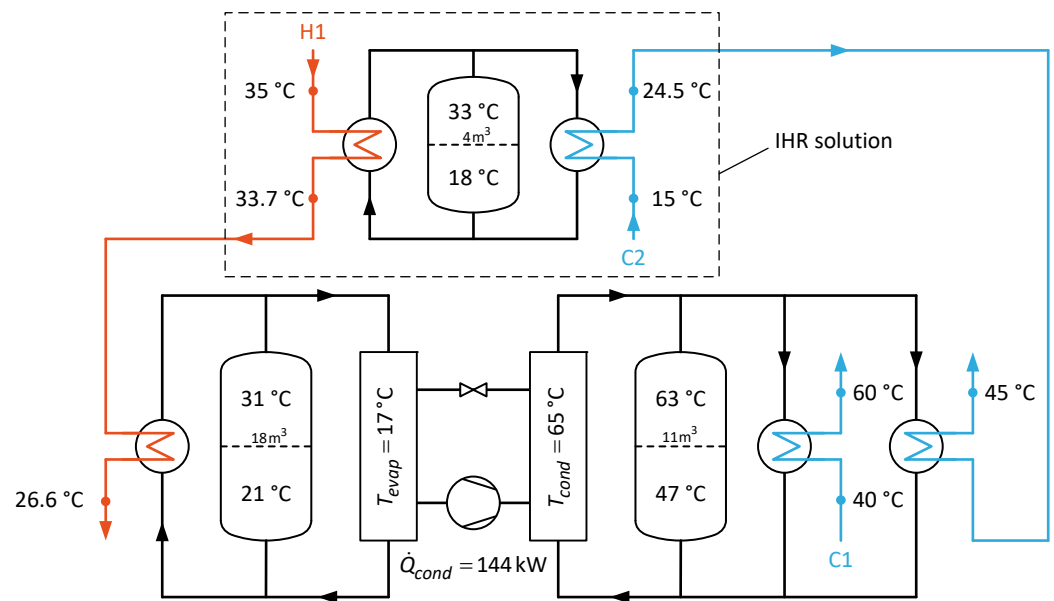


Figure 8. Schematic of solution for Variant 2: Split IHR and HP system with IHR of 80 kWh, including solution for Variant 1 highlighted as the IHR solution.

4.1.3. Indirect Heat Recovery Solution with Split HPTES System (Step 5)

After taking the residuals of the streams from the IHR, the potential HP condenser capacity according to the inverted residual ISSP (Figure 4b) is 575 kWh/batch, a 48 K temperature increase. For a split IHR and HPTES (Steps 5a and 5b) with an IHR overlap of 80 kWh, the resulting design (Variant 2) is shown in Figure 8. Three storage tanks are implemented, and the IHR storage on top is used to preheat C2 and cool H1. The HP is embedded between the two lower storage units, which are used to balance out the temporal imbalance between of the heating and cooling requirements and the continuously operating HP.

4.1.4. Combined Indirect Heat Recovery and HPTES System (Step 6)

Figure 9 shows the resulting design for the combined IHR and HP system with the same IHR of 80 kWh (Variant 3). For the HP placement in the combined system, the adapted GCC with the AZ information, shown in Figure 7, is used to identify the possible HP duty and temperature levels. With a shifted evaporation temperature of $T_{evap}^* = 21^\circ\text{C}$ and the maximum condenser duty, the resulting system has four AZs and the region with higher evaporation temperature where a fifth AZ would be necessary can be avoided. Two storage units are therefore sufficient to achieve IHR and HP integration. Comparing the GCC against the proposed adapted GCC in Figure 5, the potential reduction in the temperature increase of the HP amounts to approximately 13 K.

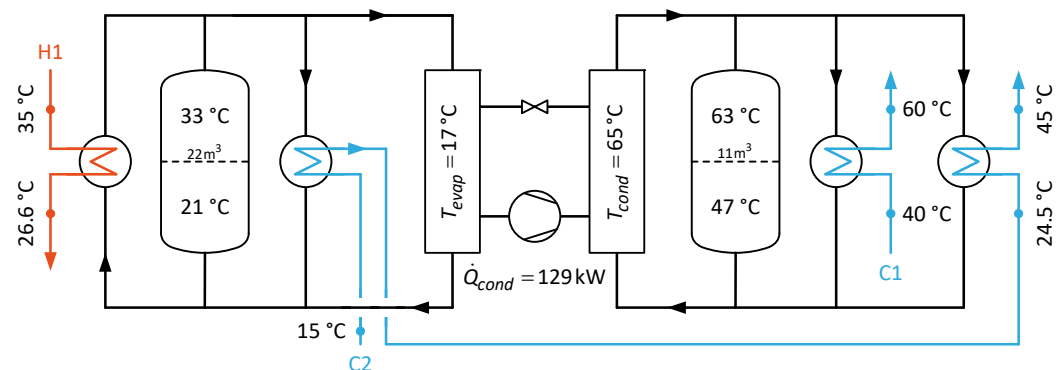


Figure 9. Schematic of Solution Variant 3: Combined IHR and HP system with IHR of 80 kWh.

4.1.5. Variant Evaluation (Step 7)

The column for “Existing Plant” is the current situation of the plant with no direct HR. The resulting investment and energy costs of the IHR system (Variant 1) and the HP integrated split (Variant 2) and combined systems (Variant 3) are shown in Table 6. Variant 1 requires low investment and has a short static payback period of 2.8 year. The annual energy cost, and thus the TAC, can be further reduced with the integration of an HP. While both HP solutions are identical from an energy perspective, they differ in terms of investment cost and system complexity. The combined system (Variant 3) is slightly less expensive due to its smaller total storage volume and smaller number of HEXes. For the combined system, an investment of approximately CHF 300,000 leads to energy cost savings of approximately CHF 70,000/y, resulting in a static payback period of 4.5 year. With an assumed operation of 15 year, an internal rate of return (IRR) of 20.7% can be achieved. Case 1 shows a significant difference only in terms of HEX area and TES volume when comparing the HP-integrated variants (Variants 2 and 3) against the IHR-only variant (Variant 1). The required TES volume is identical, and the HEX areas differ only marginally between Variants 2 and 3. Based on the results in Table 6, the decision as to which solution variant should be implemented lies with the engineers and the management. While engineering judgment in the comparison of the different solution variants is necessary (Step 7), on the whole the results favour the combined system.

Table 6. Comparison of the energy demand, cost and economic performance of the two variants.

		Existing Plant	IHR Only (Variant 1)	Split System (Variant 2)	Combined System (Variant 3)
HP Electricity demand	[MWh/year]	-	-	223	223
HU demand	[MWh/year]	983	773	0	0
CU demand	[MWh/year]	907	697	147	147
Investment cost	[CHF]	-	34,000	317,000	305,000
HP Electricity cost	[CHF/year]	-	.	26,700	26,700
HU cost	[CHF/year]	78,600	69,000	0	0
CU cost	[CHF/year]	18,100	15,700	2900	2900
Annual energy cost	[CHF/year]	96,700	84,700	29,700	29,700
Number of HEX	[-]	-	2	5	4
Total HEX area	[m ²]	-	14	110	119
Number of TES	[-]	-	1	3	2
Total TES volume	[m ³]	-	4	33	33
Total annual cost	[CHF/year]	96,700	89,300	72,800	71,100
Static payback	[year]	-	2.8	4.7	4.5
15 y IRR	[%]	-	35.3	19.7	20.7

4.2. Case 2: Industry Case Study

4.2.1. Data Extraction and Direct Heat Recovery (Steps 1 and 2)

Data extraction in this case leads to the process stream table (Table 3). As can be seen from the stream table, there are streams where the inlet conditions vary over time. This is due to pre-implemented direct HR (Step 1). The residual energy demands remaining following the pre-implemented direct HR measures are then used for further analysis.

4.2.2. Indirect Heat Recovery Possibilities (Step 3)

The required heating and cooling with the implemented direct HR before IHR is 7231 kWh/day and 7050 kWh/day, respectively. The utility cost associated with these measures is 216 kCHF/y before any IHR integration.

The first step needed for the analysis of a process using ISSP is to set the parameters of Equation (1) for the case. Initial analysis shows that the bandwidth exponent, y , should be altered from its default value, as there are streams with short duration (mainly cottage cheese washwater) which would otherwise limit the storage temperatures of the overall system drastically. The case is thus analysed with $y = 0.2$.

When analysing the resulting ISSP with the AZs, different points of interest in terms of IHR overlap exist. It can be identified that if IHR is increased above the following values, certain changes in the topology will occur:

- Above 700 kWh, the AZs are drastically limited in their temperature difference, influencing the final investment cost;
- At 1700 kWh, additional AZs are needed to extend the IHR, leading to an increase in the complexity of the resulting system.

Based on these limits, different IHR overlaps were selected for analysis. Figure 10 shows the ISSP for the three selected overlaps of 700 kWh, 1700 kWh, and 2000 kWh. The maximum IHR potential identifiable in the ISSP is 2400 kWh/day. The ISSP shows that all heat sinks and sources for this case are between 10 °C to 45 °C.

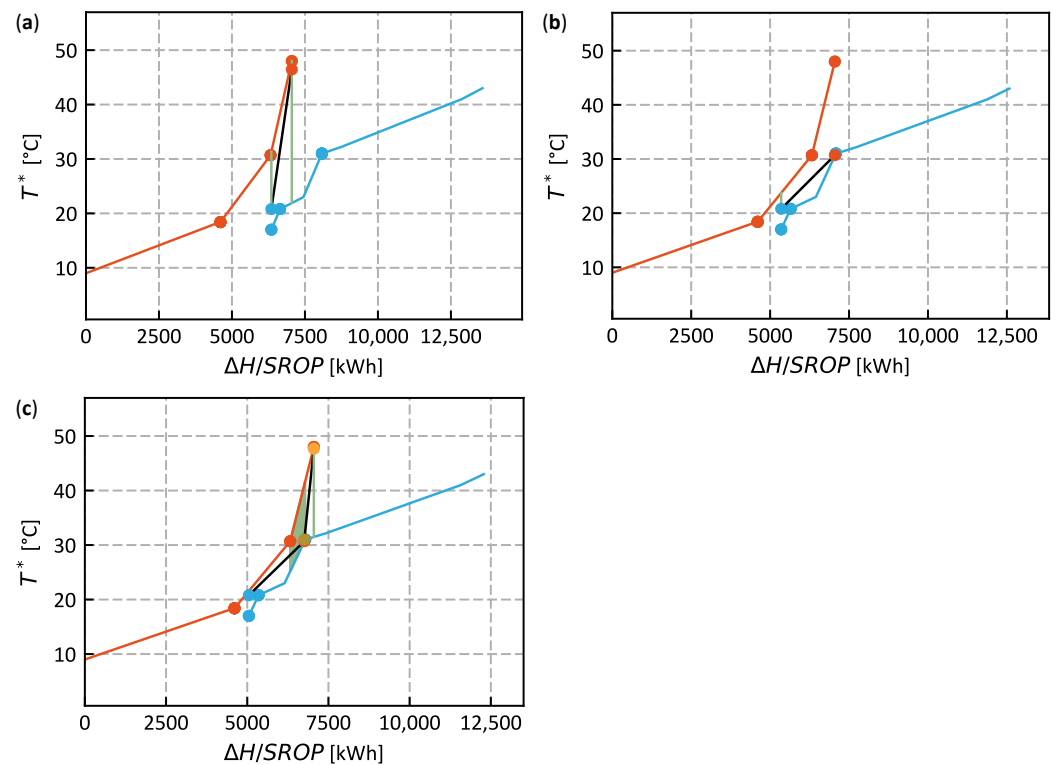


Figure 10. ISSP of Industry Case Study with IHR of (a) 700 kWh, (b) 1700 kWh, and (c) 2000 kWh, with two AZs, two AZs, and four AZs, respectively.

4.2.3. Initial Indirect Heat Recovery Solution (Step 4)

Based on the resulting numbers of AZ for the different IHR overlaps, 1700 kWh was taken as the initial solution for the evaluation of a split system setup. Figure 11 shows the schematics of the TES system for an IHR of 1700 kWh (Variant 1). As shown in Olsen et al. [26], the design of the resulting system is automatically obtained with the use of the ISSP.

The economic performance and energy demand are presented in Table 7.

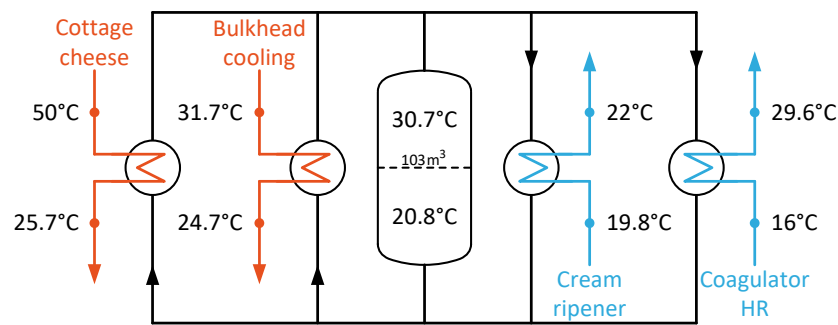


Figure 11. Schematic of solution Variant 1 of Case 2: IHR system with IHR of 1700 kWh.

Table 7. Comparison of energy, cost, and economic performance of the different variants in Case 2.

		Existing Plant	IHR Only (Variant 1)	Split System with IHR (Variant 2)	Split System without IHR (Variant 3)	Combined System (Variant 4)
HP Electricity demand	[MWh/year]	-	-	475	636	526
HU demand	[MWh/year]	2451	1875	0	0	0
CU demand	[MWh/year]	1963	1732	414	575	465
Investment cost	[CHF]	-	280,000	767,000	659,000	703,000
HP Electricity cost	[CHF/year]	-	-	53,000	71,000	58,000
HU cost	[CHF/year]	157,000	120,000	0	0	0
CU cost	[CHF/year]	59,000	52,000	12,000	14,000	14,000
Annual energy cost	[CHF/year]	216,000	172,000	65,000	85,000	72,000
Number of HEX	[-]	-	4	9	6	7
Total HEX area	[m ²]	-	258	471	249	448
Number of TES	[-]	-	1	3	2	2
Total TES volume	[m ³]	-	103	204	183	177
Total annual cost	[CHF/year]	216,000	210,000	169,000	174,000	168,000
Static payback	[year]	-	6.4	5.1	5.0	4.9
15 y IRR	[%]	-	13.2	18.0	18.3	18.9

4.2.4. Indirect Heat Recovery Solution with Split HPTES System (Step 5)

After selecting and designing the IHR system with an IHR of 1700 kWh, the remaining energy demands are extracted from the stream table. Figure 12a shows the inverted residual ISSP with 1700 kWh IHR extracted. In Figure 12a, it can be seen that the remaining heat sinks amount to approximately 5800 kWh. The figure shows that the heat sinks can be potentially supplied by an HP with 5800 kWh of condenser duty at a minimal shifted temperature of about 42 °C.

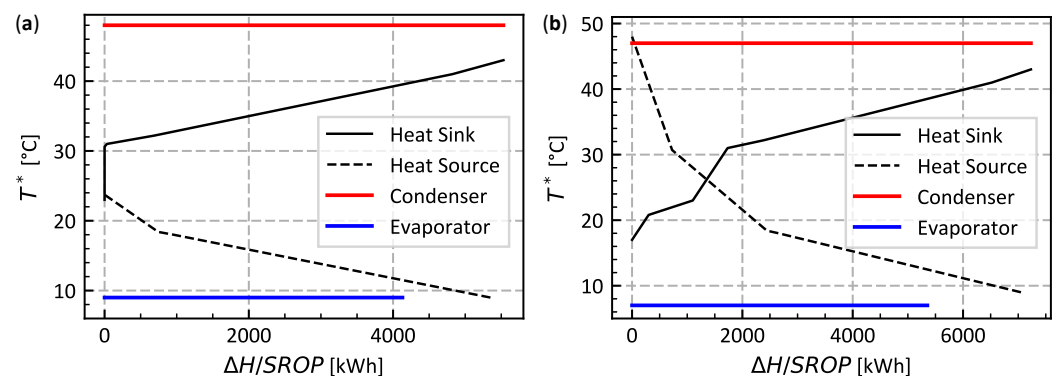


Figure 12. Inverted Residual ISSP of the industry case study for an IHR of (a) 1700 kWh and (b) 0 kWh.

Another alternative in Step 5 is to consider the split system without any IHR (i.e., an additional initial solution) and the combined system. Figure 12b shows the inverted residual ISSP without any IHR. The overlap of the heat sink and heat source in the inverted residual ISSP shows that there is unexploited IHR potential. Figure 12b shows that the HP potential is approximately 7200 kWh/day at the condenser.

Based on the inverted residual ISSP in Figure 12a, a shifted condenser temperature of approximately 48 °C and shifted evaporator temperature of 9 °C were selected. Based on this, the HPTES design for this HP placement (Variant 2) is shown in Figure 13.

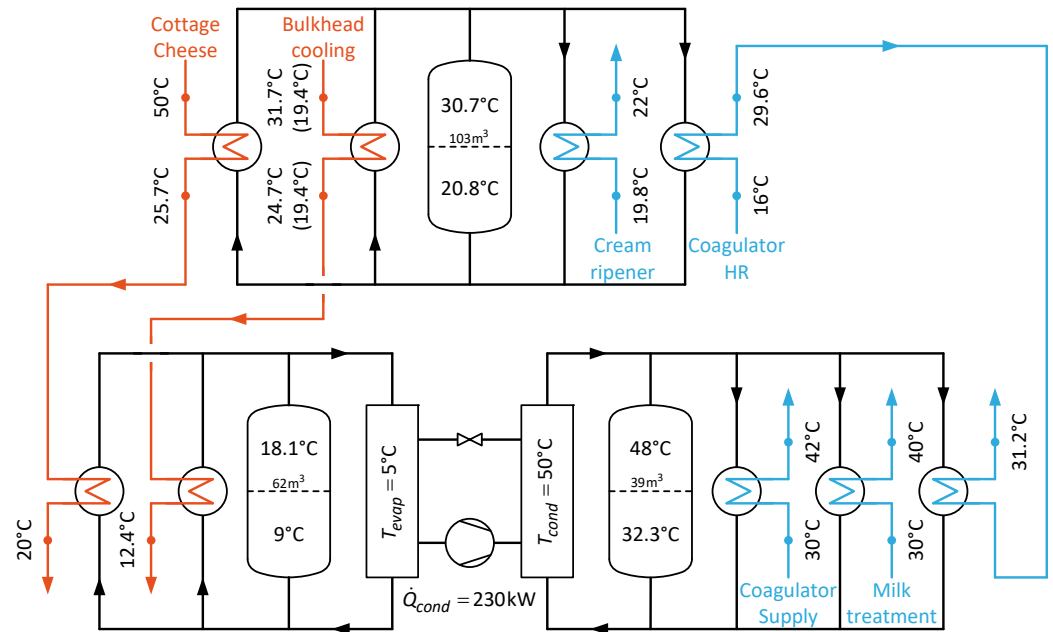


Figure 13. Schematic of solution Variant 2: Split IHR and HP system with 1700 kWh IHR.

The top half of the schematic in Figure 13 shows the IHR solution from Figure 11, and the bottom half of shows the integration of the HP and its corresponding storage system. The hot streams discharge to the evaporator side of the HP. The temperatures are then increased with a 230 kW HP to provide the heating required for the cold streams on the right. The splitting of the system leads to three TES, which are interlinked through the streams. This interlinked TES system can pose challenges concerning energy management and the controllability of the system.

Considering the alternative with no IHR, Figure 14 shows the corresponding schematics for the HPTES system (Variant 3).

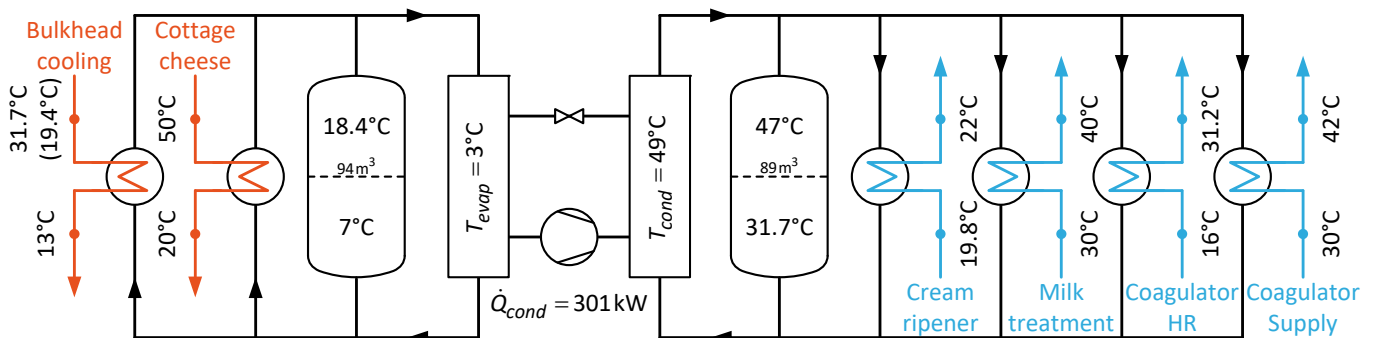


Figure 14. Schematic of solution Variant 3: HP system with no IHR at all (all HR through the HP).

Comparing Figure 14 with Figure 13, a simpler system can be obtained using two storage units which are bigger; in this system, there is no interlinking of the storages through the process streams. The same two hot streams discharge to the evaporator side of the HP, and the HP increases the temperature level to provide all the heating. The drawback of this is a larger HP with 301 kW condenser duty. Based on the number of TES and the absence of interlinking storages, the user may prefer this implementation due to its reduced complexity. However, the temperature range of the cottage cheese washing water, beginning at 50 °C, can be exploited through IHR in a combined system.

4.2.5. Combined IHR and HPTES System (Step 6)

The aim of the combined system is to search for a simpler system with the minimum number of storage units. At this stage, the user has to look at both the degree of overlaps (Figure 10) and the schematics as well as the cost associated with the final design.

For the integration of the combined HPTES system, the previously identified points of interest in terms of IHR overlap of 700, 1700, and 2000 kWh were investigated with the adapted GCC. At these points of interest there are two initial IHR solutions with only one IL and a more complicated system with four AZs where two TES are needed. The resulting adapted GCCs are shown in Figure 15.

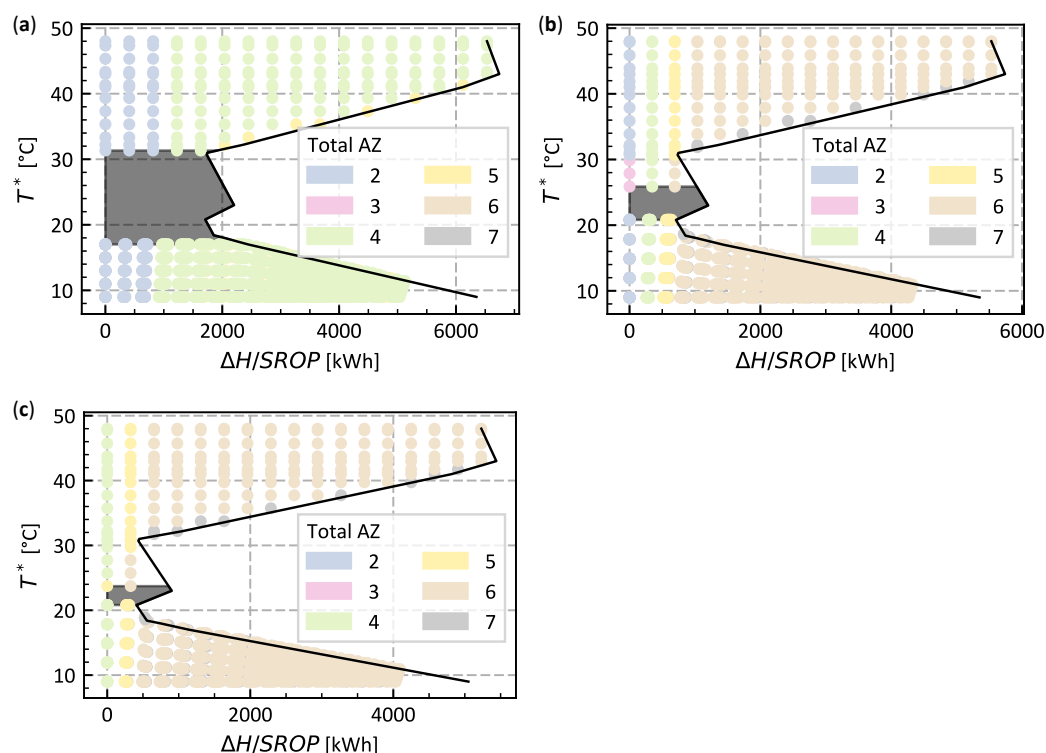


Figure 15. Adapted GCC for the industry case study with IHR of (a) 700 kWh, (b) 1700 kWh, and (c) 2000 kWh.

Based on the adapted GCC, the 700 kWh overlap configuration with four AZs appears to be the simpler system, even if the HP is placed with maximum condenser duty. In the cases with 1700 and 2000 kWh and the maximum duty, the system ends up with six AZs. However, if the condenser is placed in an unfavourable temperature region the number of AZs increases to seven. Based on Figure 15, investigation of the 700 kWh IHR solution was conducted due to the lower number of resulting AZs for any HP integration above approximately 1000 kWh condenser load. Figure 16 shows the ISSP with the HP placement with maximum condenser duty.

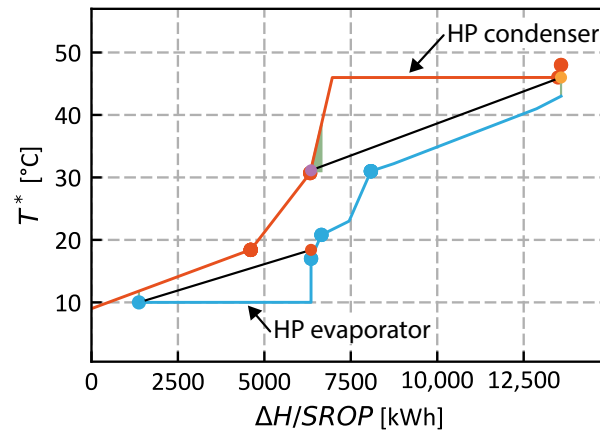


Figure 16. ISSP with the integrated HP streams for the industry case study.

The HP potential of the obtained solution in terms of condenser capacity is approximately 6500 kWh/day. The resulting ISSP with the HPTES solution contains two ILs. Figure 17 shows the schematics of the combined IHR and HPTES system (Variant 4).

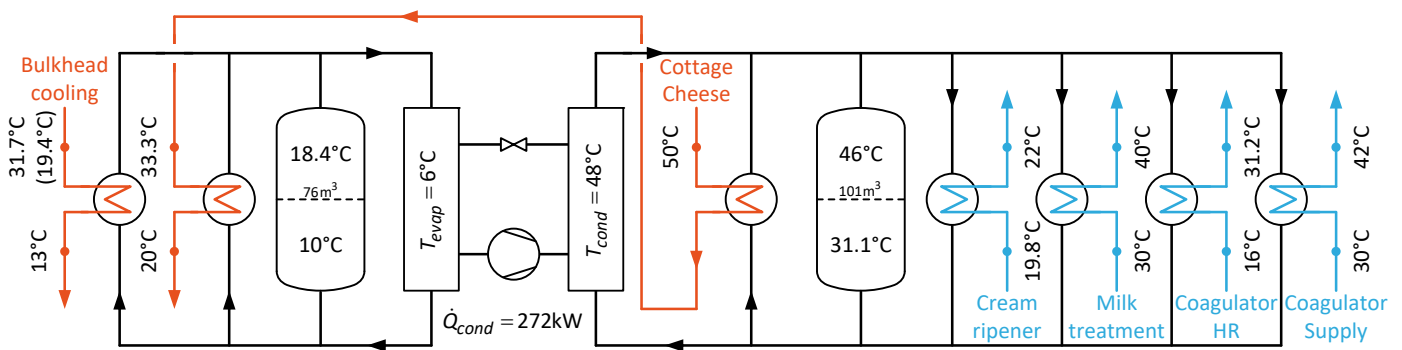


Figure 17. Schematic of solution Variant 2: Combined IHR and HP system.

The resulting system, shown in Figure 17, is similar to the split system with no IHR (Figure 14). The difference between the two systems is the better exploitation of the cottage cheese wash water. The cottage cheese wash water first discharges into the hot storage to a temperature of 33.3 °C, then discharges the remaining heat to the evaporator side of the storage system. The HP duty is reduced from 300 kW to 270 kW, resulting in lower energy and investment cost for the HP.

4.2.6. Variant Evaluation (Step 7)

Table 7 shows the comparison of the different variants in terms of energy demands, cost, and economic performance. The numbers of TES and HEX are used to measure the complexity of the systems.

The column “Existing plant” represents the current situation with direct HR already implemented. Variant 1 is used as the reference for comparison. With the previously implemented measures the TAC is at 216 kCHF/y. With the integration of an HP in the combined system, the TAC is reduced to 168 kCHF/y, which is a reduction of 22%. The investment cost of the variants ranges from approximately 660 to 770 kCHF for HP, TES, and HEX networks. With a potential energy cost reduction of about 2/3, the saving potential is significant. The static paybacks for the three HP-integrated variants are interesting, at approximately 5 y. Solely based on the economics, Variants 2, 3, and 4 are comparable. However, in terms of system complexity the design of the combined system is simpler than the split system, as indicated by the lower number of storage units and HEXes needed. The lowest complexity is achieved with Variant 3, although with the downside of the highest remaining energy cost. While the storage volumes for the HP-integrated Variants 2, 3, and 4

vary only marginally, the HEX areas vary significantly, with a pronounced minimum in Variant 3. Users have to decide whether to implement the system with the lowest TAC or with the same TAC more complexity, and better longer-term performance. Based on the results in Table 7, Variants 3 and 4 are the most favorable for implementation.

5. Discussion

HP integration in industry faces multiple challenges which have prevented widespread adoption of the technology. In particular, the non-continuous nature of many industrial processes poses additional challenges due to different process schedules or changing process requirements. Furthermore, to enhance adoption rates in industry engineers need practical tools that can be applied with an acceptable level of effort. This paper developed a workflow which provides a guideline for engineers to follow in a systematic way when integrating HPs and TES systems into non-continuous processes. The workflow allows the selection of either of two pathways for the integration of HP: (i) an HPTES system separate from the HESN, and (ii) a combined HPTES integrated with an HESN. For the former separate system, an inverted residual ISSP is derived where the source profile (hot composite curve) is inverted in its enthalpy coordinates. In the latter pathway, a novel adapted GCC based on the ISSP is developed to provide information on the impact of HP placement on system complexity. The adapted GCC shows the resulting number of AZs for a corresponding condenser and evaporator placement scheme. Following the developed W+workflow, shown in Figure 2, the user is guided on how to apply pre-existing and newly-derived graphical tools to evaluate different solution variants. An engineer thus does not require detailed training in the derivation or programming of such tools, and can instead focus on how to best apply them.

The above methodology was applied to two case studies. In addition to the initial demonstration case, a typical Swiss industrial process in the food industry was analysed. By integrating HPTES into the case study system, the HU was eliminated and the CU reduced by approximately 67%. The economic performance results of the variants with HPTES systems were similar, with a reduction in the TAC of approximately 22%. While the number of units required provides an indication of the resulting system complexity, engineering judgment remains important in successfully choosing the right variant. The analysed case studies show that HP integration into non-continuous processes is economically interesting; the energy consumption of the processes can be reduced drastically, with a static payback of averagely 5 year. For the industrial case study based in Switzerland, the static payback is considered economical. As a rule of thumb, an economically viable payback period for energy infrastructure (HPs) can be up to 8 years [35]. However, future work could include the development of implementation strategies to provide the user with information regarding which to energy infrastructure to implement first, e.g., HP, or TES, as a payback period of 8 years is considered high in other countries. Regarding further research, the manual method of evaluating the investment cost of the resulting systems may be subject of future research. The application of appropriate optimization methods to facilitate and enable larger-scale variant evaluation would be advisable. Furthermore, a trade-off between HP capacity and storage volume could be investigated, as the current assumption of continuous HP operation may lead to larger storage volume requirements than are optimal.

Author Contributions: Conceptualization, B.W. and R.A.; methodology, R.A., B.H.Y.O., J.A.S., P.K. and B.W.; software, R.A.; validation, R.A. and B.H.Y.O.; formal analysis, R.A.; investigation, R.A. and B.H.Y.O.; resources, B.W.; data curation, R.A.; writing—original draft preparation, R.A. and B.H.Y.O.; writing—review and editing, R.A., B.H.Y.O., J.A.S., P.K. and B.W.; visualization, R.A.; supervision, B.W.; project administration, B.W. and R.A.; funding acquisition, B.W., J.A.S. and R.A. All authors have read and agreed to the published version of the manuscript.

Funding: This research was funded by the Swiss Federal Office of Energy SFOE, contract number SI/501822-01. The APC was funded by the Lucerne University of Applied Sciences and Arts.

Institutional Review Board Statement: Not applicable.

Informed Consent Statement: Not applicable.

Data Availability Statement: The data presented in this study are available in the article.

Conflicts of Interest: The authors declare no conflict of interest. The funders had no role in the design of the study; in the collection, analyses, or interpretation of data; in the writing of the manuscript, or in the decision to publish the results.

Abbreviations

The following abbreviations are used in this manuscript:

AZ	Assignment Zone
CC	Composite Curve
GCC	Grand Composite Curve
HEN	Heat Exchanger Network
HESN	Heat Exchanger and Storage Network
HEX	Heat Exchanger
HP	Heat Pump
HPTES	Heat Pump with Thermal Energy Storage
HR	Heat Recovery
IHR	Indirect Heat Recovery
IRR	Internal Rate of Return
ISSP	Indirect Source Sink Profile
MINLP	Mixed-Integer Nonlinear Problem
PA	Pinch Analysis
SROP	Streamwise Repeated Operation Period
TAC	Total Annual Cost
TAM	Time Average Model
TES	Thermal Energy Storage
TSM	Time Slice Model
VSU	Volume Storage Unit

References

1. Townsend, D.W.; Linhoff, B. Heat and Power Networks in Process design: Part 1: Criteria for Placement of Heat Engines and Heat Pumps in Process Networks. *AIChE J.* **1983**, *29*, 742–748. [[CrossRef](#)]
2. Hindmarsh, E.; Boland, D.; Townsend, D. Heat Integrate Heat Engines in Process Plants. In Proceedings of the Eight Annual Industrial Energy Technology Conference, Richardson, TX, USA, 5–8 May 1986; Energy Systems Laboratory: Houston, TX, USA, 1986; pp. 477–489.
3. Wallin, E.; Franck, P.; Berntsson, T. Heat pumps in industrial processes—An optimization methodology. *Heat Recovery Syst. CHP* **1990**, *10*, 437–446. [[CrossRef](#)]
4. Wallin, E.; Berntsson, T. Integration of Heat Pumps in Industrial Processes. *Heat Recovery Syst. CHP* **1994**, *14*, 287–296. [[CrossRef](#)]
5. Benstead, R.; Sharman, F. Heat Pumps and Pinch Technology. *Heat Recovery Syst. CHP* **1990**, *10*, 437–446. [[CrossRef](#)]
6. Kapustenko, P.O.; Ulyev, L.M.; Boldyryev, S.A.; Garev, A.O. Integration of a heat pump into the heat supply system of a cheese production plant. *Energy* **2008**, *33*, 882–889. [[CrossRef](#)]
7. Pavlas, M.; Stehlík, P.; Oral, J.; Klemeš, J.; Kim, J.K.; Firth, B. Heat integrated heat pumping for biomass gasification processing. *Appl. Therm. Eng.* **2010**, *30*, 30–35. [[CrossRef](#)]
8. Olsen, D.; Abdelouadoud, Y.; Liem, P.; Hoffmann, S.; Wellig, B. Integration of Heat Pumps in Industrial Processes with Pinch Analysis. In Proceedings of the 12th IEA Heat Pump Conference, Rotterdam, The Netherlands, 15–18 May 2017.
9. Schlosser, F.; Wiebe, H.; Walmsley, T.G.; Atkins, M.J.; Walmsley, M.R.W.; Hesselbach, J. Heat Pump Bridge Analysis Using the Modified Energy Transfer Diagram. *Energies* **2020**, *14*, 137. [[CrossRef](#)]
10. Walmsley, M.R.W.; Lal, N.S.; Walmsley, T.G.; Atkins, M.J. A Modified Energy Transfer Diagram for Heat Exchanger Network Retrofit Bridge Analysis. *Chem. Eng. Trans.* **2017**, *61*, 907–912. [[CrossRef](#)]
11. Atkins, M.J.; Walmsley, M.R.; Neale, J.R. The challenge of integrating non-continuous processes—Milk powder plant case study. *J. Clean. Prod.* **2010**, *18*, 927–934. [[CrossRef](#)]

12. de Boer, R.; Smeding, S.; K, B. Waste heat recovery in industrial batch processes: Analysis of combined heat storage and heat pump application. In Proceedings of the 12th IEA Heat Pump Conference, Rotterdam, The Netherlands, 15–18 May 2017.
13. Schlosser, F.; Seevers, J.P.; Peesel, R.H.; Walmsley, T.G. System efficient integration of standby control and heat pump storage systems in manufacturing processes. *Energy* **2019**, *181*, 395–406. [[CrossRef](#)]
14. Glembin, J.; Büttner, C.; Steinweg, J.; Rockendorf, G. Thermal storage tanks in high efficiency heat pump systems—Optimized installation and operation parameters. *Energy Procedia* **2015**, *73*, 331–340. [[CrossRef](#)]
15. Floss, A.; Hofmann, S. Optimized integration of storage tanks in heat pump systems and adapted control strategies. *Energy Build.* **2015**, *100*, 10–15. [[CrossRef](#)]
16. Lambauer, J.; Fahl, U.; Ohl, M.; Blesl, M. Large scale industrial heat pump – market analysis, potentials, barriers and best—Practice examples. In Proceedings of the 9th IEA Heat Pump Conference, Zürich, Switzerland, 20–22 May 2008.
17. Becker, H.; Vuillermoz, A.; Maréchal, F. Heat Pump Integration in a Cheese Factory. *Appl. Therm. Eng.* **2012**, *43*, 118–127. [[CrossRef](#)]
18. Becker, H.; Girardin, L.; Maréchal, F. Energy integration of industrial sites with heat exchange restrictions. *Comput. Aided Chem. Eng.* **2010**, *28*, 1141–1146. [[CrossRef](#)]
19. Becker, H.; Maréchal, F. Targeting industrial heat pump integration in multi-period problems. *Comput. Aided Chem. Eng.* **2012**, *31*, 415–419. [[CrossRef](#)]
20. Schlosser, F.; Arpagaus, C.; Walmsley, T.G. Heat Pump Integration by Pinch Analysis for Industrial Applications: A Review. *Chem. Eng. Trans.* **2019**, *76*, 7–12. [[CrossRef](#)]
21. Prendl, L.; Schenzel, K.; Hofmann, R. Simultaneous integration of heat pumps and different thermal energy storages into a tightened multi-period MILP HENS superstructure formulation for industrial applications. *Comput. Chem. Eng.* **2021**, *147*, 107237. [[CrossRef](#)]
22. Beck, A.; Hofmann, R. A Novel Approach for Linearization of a MINLP Stage-Wise Superstructure Formulation. *Comput. Chem. Eng.* **2018**, *112*, 17–26. [[CrossRef](#)]
23. Prendl, L.; Hofmann, R. An Extended Approach for the Integration of Heat Pumps into HENS Multi-Period MILP Superstructure Formulation for Industrial Applications. *Comput. Aided Chem. Eng.* **2020**, *48*, 1351–1356. [[CrossRef](#)]
24. Stampfli, J.A.; Atkins, M.J.; Olsen, D.G.; Walmsley, M.R.; Wellig, B. Practical heat pump and storage integration into non-continuous processes: A hybrid approach utilizing insight based and nonlinear programming techniques. *Energy* **2019**, *182*, 236–253. [[CrossRef](#)]
25. Linnhoff, B.; Ashton, G.; Obeng, E. *Process Integration of Batch Processes*; AiChE Annual Meeting: New York, NY, USA, 1988.
26. Olsen, D.; Abdelouadoud, Y.; Wellig, B.; Krummenacher, P. Systematic thermal energy storage integration in industry using pinch analysis. In Proceedings of the 29th International Conference on Efficiency, Cost, Optimization, Simulation and Environmental Impact of Energy Systems, Portoroz, Slovenia, 19–23 June 2016; pp. 1–14.
27. Krummenacher, P.; Favrat, D. Indirect and mixed direct-indirect heat integration of batch processes based on Pinch analysis. *Int. J. Appl. Thermodyn.* **2001**, *4*, 135–143.
28. Walmsley, T.G.; Walmsley, M.R.; Atkins, M.J.; Neale, J.R. Integration of industrial solar and gaseous waste heat into heat recovery loops using constant and variable temperature storage. *Energy* **2014**, *75*, 53–67. [[CrossRef](#)]
29. Abdelouadoud, Y.; Lucas, E.; Krummenacher, P.; Olsen, D.; Wellig, B. Batch process heat storage integration: A simple and effective graphical approach. *Energy* **2019**, *185*, 804–818. [[CrossRef](#)]
30. Linnhoff, B.; Hindmarsh, E. The Pinch design method for heat-exchanger networks. *Chem. Eng. Sci.* **1983**, *38*, 745–763. [[CrossRef](#)]
31. Klemeš, J.J.; Varbanov, P.S. Implementation and pitfalls of process integration. *Chem. Eng. Trans.* **2010**, *21*, 1369–1374. [[CrossRef](#)]
32. Brunner, F.; Krummenacher, P. *Einführung in Die Prozessintegration Mit der Pinch-Methode, Handbuch für Die Analyse von Kontinuierlichen Prozessen und Batch-Prozessen*; Bundesamt für Energie: Bern, Switzerland, 2017; pp. 1–175.
33. Townsend, D.W.; Linnhoff, B. Heat and Power Networks in Process design: Part 2: Design procedure for Equipment Selection and process matching. *AIChE J.* **1983**, *29*, 748–771. [[CrossRef](#)]
34. Rast, L. Development of Equipment Module and Investment Cost Estimating Functions and Integration Concept in the PinCH Software. Master's Thesis, Lucerne University of Applied Sciences and Arts, Lucerne, Switzerland, 2018.
35. Abteilung Klima. *CO₂-Abgabebefreiung Ohne Emissionshandel*; Technical Report; Bundesamt für Umwelt: Bern, Switzerland, 2019.